## ORIGINAL ARTICLE

# Rac-mediated actin remodeling and myosin II are involved in $K_{ATP}$ channel trafficking in pancreatic β-cells

Young-Eun Han[1], Ajin Lim[1], Sun-Hyun Park[1], Sunghoe Chang, Suk-Ho Lee and Won-Kyung Ho

**AMP-activated protein kinase (AMPK) is a metabolic sensor activated during metabolic stress and it regulates various enzymes and cellular processes to maintain metabolic homeostasis. We previously reported that activation of AMPK by glucose deprivation (GD) and leptin increases $K_{ATP}$ currents by increasing the surface levels of $K_{ATP}$ channel proteins in pancreatic β-cells. Here, we show that the signaling mechanisms that mediate actin cytoskeleton remodeling are closely associated with AMPK-induced $K_{ATP}$ channel trafficking. Using F-actin staining with Alexa 633-conjugated phalloidin, we observed that dense cortical actin filaments present in INS-1 cells cultured in 11 mM glucose were disrupted by GD or leptin treatment. These changes were blocked by inhibiting AMPK using compound C or siAMPK and mimicked by activating AMPK using AICAR, indicating that cytoskeletal remodeling induced by GD or leptin was mediated by AMPK signaling. AMPK activation led to the activation of Rac GTPase and the phosphorylation of myosin regulatory light chain (MRLC). AMPK-dependent actin remodeling induced by GD or leptin was abolished by the inhibition of Rac with a Rac inhibitor (NSC23766), siRac1 or siRac2, and by inhibition of myosin II with a myosin ATPase inhibitor (blebbistatin). Immunocytochemistry, surface biotinylation and electrophysiological analyses of $K_{ATP}$ channel activity and membrane potentials revealed that AMPK-dependent $K_{ATP}$ channel trafficking to the plasma membrane was also inhibited by NSC23766 or blebbistatin. Taken together, these results indicate that AMPK/Rac-dependent cytoskeletal remodeling associated with myosin II motor function promotes the translocation of $K_{ATP}$ channels to the plasma membrane in pancreatic β-cells.**

## INTRODUCTION

Pancreatic β-cells have important roles in maintaining glucose homeostasis by secreting insulin in response to elevated blood glucose levels.[1] The $K_{ATP}$ channel is found in brain, heart, smooth muscle and pancreatic β-cells, and serves as a bridge between glucose metabolism and the electrical activity of pancreatic β-cells. Of note, it is well accepted that ATP-dependent gating is a key mechanism of how $K_{ATP}$ channels couple blood glucose levels to the membrane potentials of pancreatic β-cells. However, we have recently presented evidence that $K_{ATP}$ channel activity and the resting membrane potential of pancreatic β-cells are closely correlated with the activity of AMP-activated protein kinase (AMPK) and that AMPK increases $K_{ATP}$ channel density by promoting $K_{ATP}$ channel trafficking to the cell surface.[2] Because AMPK is activated not only by energy deprivation[3] but also by receptor-mediated signaling such as leptin via $Ca^{2+}$/calmodulin

kinase kinase activation, even at normal or high glucose concentrations,[2,4] our results imply that the surface density of $K_{ATP}$ channels regulated by AMPK, rather than the open probability of $K_{ATP}$ channels regulated by intracellular ATP concentrations, is a key determinant of the membrane potential in pancreatic β-cells. Therefore, understanding the cellular and molecular mechanisms of how the activation of AMPK leads to $K_{ATP}$ channel trafficking is a prerequisite for understanding the regulation of pancreatic β-cell excitability and insulin secretion.

AMPK has long been known to be a regulator of metabolism,[3] but many other functions of AMPK have been recognized in recent studies. The energy-dependent regulation of cell structure, which is critical for controlling cell polarity and mitosis in *Drosophila*, is mediated by AMPK, as non-muscle myosin regulatory light chain (MRLC) is a target of AMPK.[5] Vasodilator-stimulated phosphoprotein, an actin regulatory protein, was shown to be regulated by

Department of Physiology and Biomembrane Plasticity Research Center, Seoul National University College of Medicine, Seoul, Republic of Korea
[1]These authors contributed equally to this work.
Correspondence: Professor W-K Ho, Department of Physiology, Seoul National University College of Medicine, 103 Daehak-ro, Jongno-gu, Seoul 110-799, Republic of Korea.
E-mail: wonkyung@snu.ac.kr

AMPK-dependent phosphorylation, and phosphorylated vasodilator-stimulated phosphoprotein impaired actin cytoskeleton assembly in endothelial cells.[6] These results suggest that the signaling pathways downstream of AMPK link a wide range of signaling mechanisms that regulate the actin cytoskeleton, having different roles in different systems or cell types. Considering that actin and related proteins are also involved in the regulation of exocytosis,[7,8] we hypothesized that the reorganization of the actin cytoskeletal network by AMPK signaling mediates the surface trafficking of K$_{ATP}$ channels. Consistently, conditions that can activate AMPK, such as GD and leptin application, were shown to induce actin depolymerization in pancreatic β-cells.[9,10] However, the downstream targets of AMPK that mediate cytoskeletal remodeling in pancreatic β-cells remain to be elucidated.

The Rho family of small GTPases, including Cdc42, Rac and Rho, are molecular switches that regulate actin cytoskeleton organization and are also implicated in intracellular trafficking. Rac-dependent actin remodeling was shown to be crucial for the translocation of GLUT4, a glucose transporter highly expressed in muscle and adipocytes, to the plasma membrane by insulin signaling.[11] In pancreatic β-cells, Rac was reported to be involved in insulin granule exocytosis.[12,13] Myosin II, the conventional myosin first studied for its role in muscle contraction, is present also in non-muscle cells, and non-muscle myosin II (MyoII) is implicated in a number of important cellular processes including the active assembly/disassembly of cytoskeletal substructures[14–17] and trafficking of vesicles or membrane proteins.[18–20] Furthermore, a functional link between MyoII and Rac1/Cdc42 GTPases in regulating actin dynamics was reported in migrating cells[21] and neuronal growth cones.[22] Together, these observations suggest the possibility that Rac GTPases or MyoII may mediate AMPK-dependent actin remodeling and K$_{ATP}$ channel trafficking in pancreatic β-cells. In the present study, we investigated this possibility using INS-1 cells. We employed various techniques to assess K$_{ATP}$ channel trafficking: immunocytochemistry to visualize the subcellular distribution of the proteins, biotinylation assays for the quantification of surface proteins, and electrophysiological analysis for confirmation that the channels are indeed fused to the membrane and that their activity contributes to cellular excitability.

## MATERIALS AND METHODS
### Cell culture
Rat insulinoma INS-1 cells (passage 20–50) were cultured as previously described.[4] Cells were cultured in RPMI 1640 medium (Sigma, St Louis, MO, USA) containing 11.1 mM D-glucose supplemented with 10% heat-inactivated fetal bovine serum, 10 mM HEPES, 100 units ml$^{-1}$ penicillin, 100 μg ml$^{-1}$ streptomycin, 1 mM sodium pyruvate and 50 μM β-mercaptoethanol in a humidified incubator supplied with 5% $CO_2$ at 37 °C. Cells were grown in 12-well plates at a density of $5 \times 10^4$ cells per well for electrophysiology, and on 12-mm poly-L-lysine-coated coverslips at $5 \times 10^4$ per coverslip for immunocytochemistry.

### Electrophysiology
K$_{ATP}$ channel currents and membrane potentials were measured with an EPC 10 amplifier and PULSE software (version 8.67; HEKA Elektronik, Lambrecht, Germany) at room temperature using inside-out patch clamp and perforated patch clamp techniques, respectively. The data were analyzed using IGOR software (Wavemetrics, Lake Oswego, OR, USA). Patch electrodes were pulled from borosilicate glass capillaries to a resistance between 3 and 4 MΩ when filled with pipette solution. For inside-out patch recordings, patch pipettes were filled with an internal solution containing the following (in mM): 140 KCl, 2.6 CaCl$_2$, 1.1 MgCl$_2$ and 10 HEPES (pH 7.2 with KOH), and a bath solution comprising (in mM): 140 KCl, 2 CaCl$_2$, 1 MgCl$_2$, 11 EGTA, 10 HEPES (pH 7.2 with KOH). The internal solution for perforated patch recordings contained the following (in mM): 110 K-aspartate, 30 KCl, 2.6 CaCl$_2$, 0.5 EGTA, 5 EDTA, 10 HEPES (pH 7.2 with KOH) and 200 μM nystatin, and the bath solution (normal Tyrode's solution) contained (in mM): 143 NaCl, 5.4 KCl, 0.5 MgCl$_2$ and 1.8 CaCl$_2$, 5 HEPES (pH 7.4 with NaOH). Single-channel K$_{ATP}$ currents were recorded at − 60 mV by inside-out patch and analyzed for channel activity ($NPo$; where $N$ is the number of functional channels, and $Po$ is the open probability).

### Immunofluorescence and confocal laser-scanning microscopy
For K$_{ATP}$ channel staining, immunofluorescence experiments were performed as described previously.[4] After fixation with 4% paraformaldehyde in phosphate-buffered saline (PBS) for 15 min and washing in PBS, cells were permeabilized with 0.25% Triton X-100 in PBS for 10 min, followed by three washes in PBS and blocking with 2% donkey serum in PBS for 30 min at room temperature. Cells were then incubated with rabbit polyclonal anti-Kir6.2 antibody (H-55, sc-20809, 1:50, Santa Cruz Biotechnology, Santa Cruz, CA, USA) overnight at 4°C, rinsed in PBS, and the subcellular localization of Kir6.2 was visualized using Alexa 488-conjugated donkey anti-rabbit IgG antibody (1:100, Invitrogen, Eugene, OR, USA). After washing, the cells were mounted with Gel Mount (Biomeda, Foster City, CA, USA) on slides. Images were acquired on a FluoView 1000 confocal microscope (Olympus, Tokyo, Japan) using a 60 or ×100 oil immersion objective or a TCS-SP2 confocal laser-scanning microscope (Leica, Heidelberg, Germany) with a 40 or ×63 water immersion objective, and processed using Olympus FV10-ASW 3.01 confocal microscopy software (Olympus) or Leica Confocal Software (Leica). To analyze K$_{ATP}$ channel distribution, fluorescence intensity profiles were measured along lines drawn across the cell, excluding the nucleus. Surface localization of Kir6.2 was measured by integration of the fluorescence intensities in the dashed line boxes at the cell periphery. For staining filamentous actin (F-actin), after fixation for 10 min, cells were permeabilized with 0.1% Triton X-100 in PBS for 5 min, extensively washed, blocked with 1% BSA in PBS for 20 min, and then incubated with Alexa Fluor 488- or Alexa Fluor 633-conjugated phalloidin (Invitrogen) for 20 min at room temperature. Images were acquired on a TCS-SP2 confocal laser-scanning microscope with a ×63 water immersion objective or a FluoView 1000 confocal microscope with a 60 or ×100 oil immersion objective, and processed using Leica Confocal Software or Olympus FV10-ASW 3.01 confocal microscopy software. The same instrument settings were used for each experiment, and all experiments were repeated at least three times.

## Surface biotinylation and western blotting

To detect cell surface Kir6.2, an EZ-Link Sulfo-NHS-SS-Biotin kit (Pierce, Rockford, IL, USA) was used as previously described.[2] The total and cell surface levels of Kir6.2 were measured using rabbit polyclonal anti-Kir6.2 antibody (1:1000). The protein samples were separated by 10–12% SDS–polyacrylamide gel and transferred onto a polyvinylidene difluoride membranes (Millipore, Temecula, CA, USA). The blotted membrane was blocked with 5% skim milk and 0.2% Tween-20 in PBS for 2 h at room temperature and incubated with rabbit polyclonal anti-Kir6.2 antibody overnight at 4°C. After washing, the membrane was incubated with secondary goat polyclonal anti-rabbit IgG-HRP (1:2500, Abcam, Cambridge, UK) for 1 h at room temperature. Detection was performed with Amersham ECL Plus western Blotting Detection Reagents (GE Healthcare, Piscataway, NJ, USA) and blots were exposed to X-ray film. Quantification of active Rac was performed using a Rac activation assay kit (Millipore) according to the manufacturer's instructions. In brief, cells were lysed in magnesium lysis buffer. Cell lysates were precleared for 10 min with glutathione beads. Lysates were then incubated with p21-activated kinase-1 (PAK-1) p21-binding domain-agarose for 1 h at 4°C. Beads were washed three times in magnesium lysis buffer, and samples were resolved by 15% SDS–polyacrylamide gel. GTP-bound Rac1 or GTP-bound Rac2 was detected by mouse monoclonal anti-Rac1 antibody (clone 23A8, 1:1000) or rabbit anti-Rac2 antiserum (Catalog # 07-604, 1:5000). The relative band intensities were compared via band scanning using a Gel Doc XR (Bio-Rad, Hercules, CA, USA) with Quantity One software, version 4.5.2 or the densitometric analysis software Multi Gauge v3.0 (Fujifilm, Tokyo, Japan).

## Small interfering RNA (siRNA)-mediated knockdown

AMPK was knocked downed by an small interfering RNA (siRNA) targeting AMPK (siAMPK), as described in our previous paper.[4] To suppress Rac1 or Rac2 expression, the silencer select siRNAs against Rac1 (siRac1: 5′-AGAUCGGUGCUGUCAAAUAtt-3′) and Rac2 (siRac2: 5′-AUGUGAUGGUGGACAGUAAtt-3′) were purchased from Ambion (Austin, TX, USA). siGFP (5′-GCAAGCUGACCC UGAAGUUCAU-3′, Qiagen, Valencia, CA, USA) or scrambled siRNA (5′-AUUGUAUGCGAUCGCAGAC-3′, Dharmacon, Lafayette, CO, USA) was used for the control siRNA (siCtrl) as described previously.[2] Cells were co-transfected with siRac1 or siRac2 and a DsRed reporter vector using Lipofectamine 2000 (Invitrogen) according to the manufacturer's instructions, and experiments were performed 48 h after transfection.

## Flow cytometry

After fixation for 10 min, cells were permeabilized with 0.5% Triton X-100 in PBS containing 0.1% BSA for 10 min, followed by blocking with 1% BSA in PBS for 20 min. Then, cells were incubated with 4 units ml$^{-1}$ Alexa 633-conjugated phalloidin for 20 min at room temperature. Stained cells were washed and analyzed using a FACScalibur (BD Bioscience, Franklin Lakes, NJ, USA).

## Statistical analysis

Data were are expressed as the mean ± s.e.m. Significant differences between the experimental groups were analyzed using unpaired two-sampled Student's *t*-tests. $P < 0.05$ was considered statistically significant.

# RESULTS

## AMPK signaling underlies actin remodeling induced by glucose deprivation and leptin

We previously reported that GD or leptin induces AMPK activation, which leads to K$_{ATP}$ channel trafficking to the plasma membrane.[2,4] In neuroendocrine cells and pancreatic β-cells where dense cortical actin is prominent, cytoskeletal remodeling has been shown to be crucial for the regulation of vesicular trafficking and hormone secretion.[7,23] To investigate the possibility that actin remodeling is involved in AMPK-dependent K$_{ATP}$ channel trafficking in pancreatic β-cells, we first examined whether GD induces actin remodeling. INS-1 cells cultured in 11 mM glucose-containing media at 37 °C were transferred to Tyrode's solutions containing 11 or 0 mM glucose at room temperature. After 2 h incubation, F-actin was stained with Alexa 633-conjugated phalloidin. In INS-1 cells incubated in 11 mM glucose, prominent cortical actin was observed, but treatment of INS-1 cells with glucose-free solution induced disruption of F-actin (Figure 1a). The effect of GD on the actin cytoskeleton was abolished by compound C (CC), an AMPK inhibitor (Figure 1a), indicating that cytoskeletal remodeling by GD is mediated by AMPK signaling. To further examine AMPK-dependent actin remodeling, we quantified changes in F-actin contents with flow cytometry. The flow profiles showed a significant decrease in F-actin in GD-treated cells compared with controls, and this decrease was blocked by compound C (Figure 1b, left) or knockdown of AMPK using siAMPK, siRNA targeted against AMPK (Figure 1b, right). Reduced expression of endogenous AMPK in siAMPK-transfected INS-1 cells was confirmed (Figure 6a). We have previously shown that treatment of INS-1 cells with AICAR, an AMPK activator, or leptin in 11 mM glucose solutions induced AMPK activation in INS-1 cells to a similar extent as that induced by a 2-h incubation in 0 mM glucose.[2,4] Consistently, AICAR (0.25 mM, for 30 min) or leptin (10 nM for 30 min) treatment in 11 mM glucose-induced marked actin disruption, as was observed in GD (Figure 1c). The effect of leptin on the actin cytoskeleton was also abolished by CC (Figure 1c). Together, these data indicate that AMPK signaling mediates the cytoskeletal remodeling induced by GD or leptin.

## AMPK-dependent actin remodeling is mediated by Rac signaling

The Rho family small GTPases (Rho, Rac, and Cdc42) are molecular switches regulating downstream events that regulate actin cytoskeleton.[24] Rac mediates cytoskeletal remodeling and GLUT4 trafficking by insulin signaling in muscles and adipocytes.[25,26] To determine whether Rac is involved in AMPK-induced actin remodeling, we evaluated the effect of a Rac inhibitor, NSC23766 in INS-1 cells. When 50 μM NSC23766 was applied during GD treatment or with 10 nM leptin, actin depolymerization did not occur and dense cortical actin was observed, suggesting the involvement of Rac in AMPK-induced actin remodeling (Figure 2a).

To determine whether Rac is indeed activated by GD, and whether this activation is AMPK-dependent, we performed a
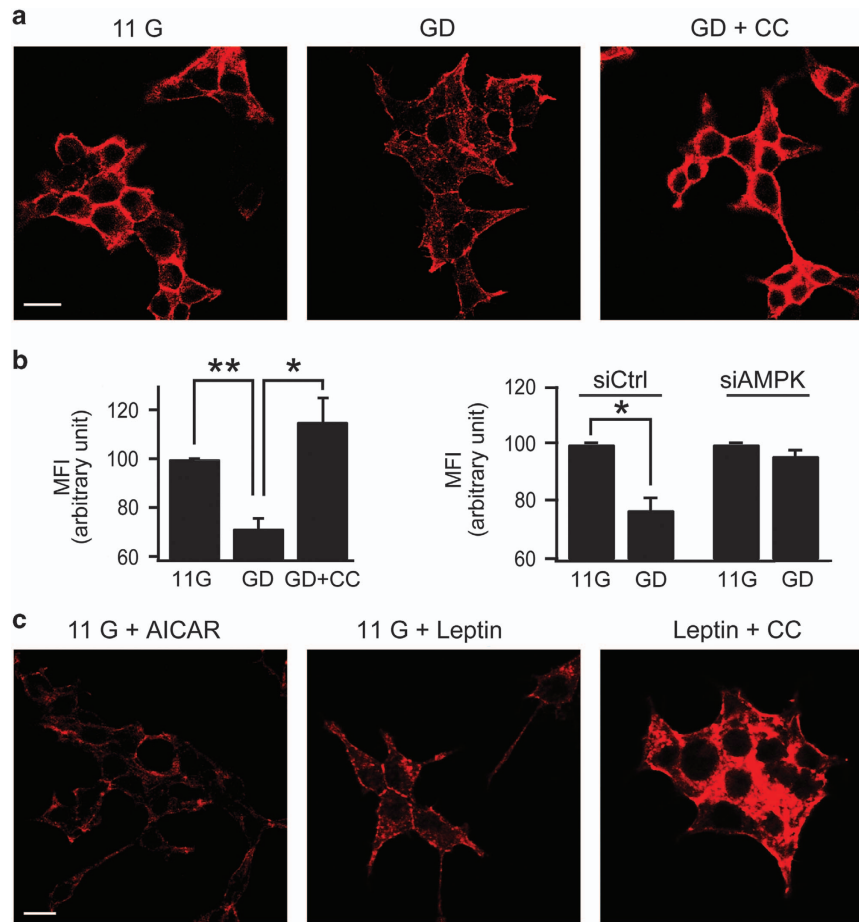
**Figure 1** Glucose deprivation or leptin induces actin disruption via AMPK signaling in INS-1 cells. (**a**, **c**) Confocal fluorescent images of INS-1 cells stained with Alexa 633-phalloidin for F-actin staining. (**a**) Before fixation, cells were pretreated with 11 mm glucose (11 G) or 0 mm glucose for 2 h in the absence (GD) or presence of 10 μm compound C (GD+CC). Scale bars, 10 μm. (**b**) Quantification of changes in F-actin content using FACS analysis. Mean fluorescence intensity (MFI) of 11G was arbitrarily set at 100% and compared with MFI of GD and GD+CC cells (left). MFI of siAMPK-transfected GD cells is compared with siCtrl-transfected GD cells (right). Data are represented as the mean ± s.e.m. of three independent experiments. *$P < 0.05$ and **$P < 0.01$. (**c**) Cells were incubated in 11 mm glucose for 30 min in the presence of 0.25 mm AICAR (11 G+AICAR) or 10 nm leptin in the absence (11 G+Leptin) and the presence of 10 μm CC (Leptin+CC). Scale bars, 10 μm.

Rac activation assay for Rac1 and Rac2 using glutathione S-transferase-PBD of p-21-activated kinase, the effector of RAC, (GST-PAK-PBD) to affinity precipitate active Rac (GTP-bound Rac) from cell lysates. We observed significantly increased levels of the GTP-bound form of Rac1 and Rac2 in GD or leptin-treated INS-1 cells (Figures 2b and c). We also confirmed that Rac1 and Rac2 were activated by AICAR application (Figure 2b). Together, these results suggest that AMPK activation by GD or leptin activates both Rac1 and Rac2.

To further confirm the involvement of Rac in AMPK-dependent actin remodeling, we examined the effects of Rac knockdown using siRNA targeting Rac1 or Rac2. We first confirmed that siRac1 and siRac2 reduced the expression of endogenous Rac1 and Rac2, respectively (Supplementary Figure 1a). For F-actin analysis, cells were cultured at a low density to easily identify individual cells transfected with siRNA. In siCtrl-transfected cells, reduced F-actin was observed

in leptin-treated cells, whereas leptin-induced changes in actin were abolished in siRac1- or siRac2-transfected cells (Supplementary Figure 1b). These results suggest that the involvement of Rac is not isoform specific but that both Rac1 and Rac2 are required for leptin-induced actin remodeling.

### Rac signaling is required for $K_{ATP}$ channel trafficking

We then investigated the relationship between AMPK/Rac-dependent actin remodeling and $K_{ATP}$ channel trafficking. INS-1 cells were stained with fluorescence-labeled antibodies to Kir6.2, and immunofluorescence analysis was performed to evaluate changes in $K_{ATP}$ channel distribution. To analyze the surface localization of $K_{ATP}$ channels, we measured fluorescence intensity profiles along a line across the cell. As previously reported,[2,4] we confirmed that Kir6.2 was randomly found in the intracellular compartments in control 11G conditions, whereas leptin or GD facilitated $K_{ATP}$ channel
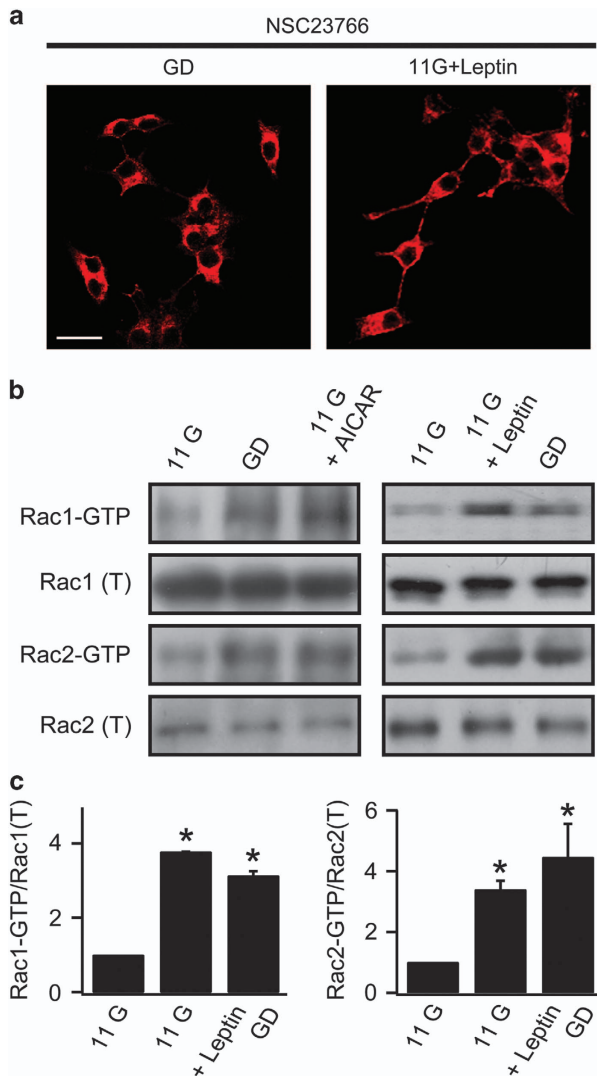
**Figure 2** Activation of Rac by AMPK signaling induced actin disruption. (**a**) Confocal fluorescent images of F-actin staining with Alexa 633-phalloidin in INS-1 cells. Cells were pretreated with 50 μM NSC23766 for 1 h in GD (left) or 30 min in 11 mM glucose during 10 nM leptin treatment (right). Scale bars, 20 μm. (**b**) Western blot analysis of Rac1 or Rac2 activity in lysates from INS-1 cells pretreated with 11 mM glucose (11 G) or glucose-deprived solution (GD) in the presence or absence of 0.25 mM AICAR (left) or 10 nM leptin (right). (**c**) Quantitative analysis of Rac activation from three independent experiments shown in (**b**). The relative ratio of activated Rac (Rac1-GTP or Rac2-GTP) to total Rac (total Rac1 or Rac2) levels was determined by band densitometry. The relative ratio in 11 G was set to 1. Data are represented as the mean ± s.e.m. of three independent experiments. *$P < 0.05$ compared with 11 G.

trafficking to the plasma membrane, resulting in a high intensity profile at the cell periphery (Figures 3a and c). Treatment of cells with phalloidin (10 μM), an actin stabilizer, inhibited K$_{ATP}$ channel trafficking to the plasma membrane induced by GD or leptin (Figures 3a and c), supporting the idea that actin remodeling is a critical step for AMPK-induced K$_{ATP}$ channel trafficking. Application of NSC23766 to

leptin- or GD-treated cells significantly inhibited K$_{ATP}$ channel trafficking to the plasma membrane, and Kir6.2 was observed randomly in the intracellular compartments (Figures 3a and c), confirming the association of Rac-induced actin remodeling and K$_{ATP}$ channel trafficking. Consistent with the involvement of Rac1 and Rac2 in actin remodeling described above (Supplementary Figure 1b), both siRac1 and siRac2 significantly inhibited leptin-induced K$_{ATP}$ channel trafficking (Figures 3b and c).

Next, to investigate the functional significance of AMPK/Rac signaling, we evaluated the effects of Rac inhibition on K$_{ATP}$ channel activity and β-cell membrane potential. We performed inside-out excised patch recordings in the presence of diazoxide (0.25 mM) and ATP (1 μM), where the open probability (Po) of K$_{ATP}$ channels was maximized. Under these conditions, changes in channel activity (NPo) represent changes in channel density (N) in the patch membrane.[4] We found that the mean value for NPo was about four times larger than in 11G-treated cells when siCtrl-transfected cells were pretreated with 10 nM leptin for 30 min, whereas leptin-induced increases in NPo were completely inhibited in cells expressing siRac1 or siRac2 (Figures 4a and b). These results indicate that knockdown of Rac1 or Rac2 completely abolished the effect of leptin on K$_{ATP}$ channel activity.

In our previous study, leptin caused significant hyperpolarization, which was mediated by the activation of K$_{ATP}$ currents.[2] To examine the effect of Rac in leptin-induced hyperpolarization, we measured resting membrane potential at 6 mM glucose using a perforated patch recording to preserve physiological conditions as much as possible. We found that 10 nM leptin failed to induce hyperpolarization in siRac1-, or siRac2-trasfected cells (Figures 4c and d). Taken together, AMPK/Rac-dependent actin remodeling is involved in regulating K$_{ATP}$ channel trafficking in pancreatic β-cells, leading to an increase in K$_{ATP}$ channel activity and membrane hyperpolarization.

## MRLC phosphorylation is involved in K$_{ATP}$ channel trafficking via AMPK signaling
Because actin remodeling by AMPK/Rac signaling was mainly mediated by actin depolymerization, we investigated whether actin depolymerization itself is sufficient to promote K$_{ATP}$ channel trafficking to the surface membrane. However, actin depolymerization by latrunculin B failed to induce K$_{ATP}$ channel trafficking or increase K$_{ATP}$ channel activity (Figures 5a and b), suggesting that actin depolymerization is a prerequisite, but not sufficient, for inducing K$_{ATP}$ channel trafficking. As a likely candidate for an additional signal that mediates AMPK-dependent K$_{ATP}$ channel trafficking associated with actin remodeling, we examined the involvement of MRLC because the phosphorylation of MRLC underlies various cellular events mediated by AMPK signaling. In particular,[5] showed that the activation of AMPK by energy deprivation induces actin polarization via the phosphorylation of MRLC, resulting in changes in cell shape. We first assessed the effect of leptin on pMRLC levels by western blotting in control and
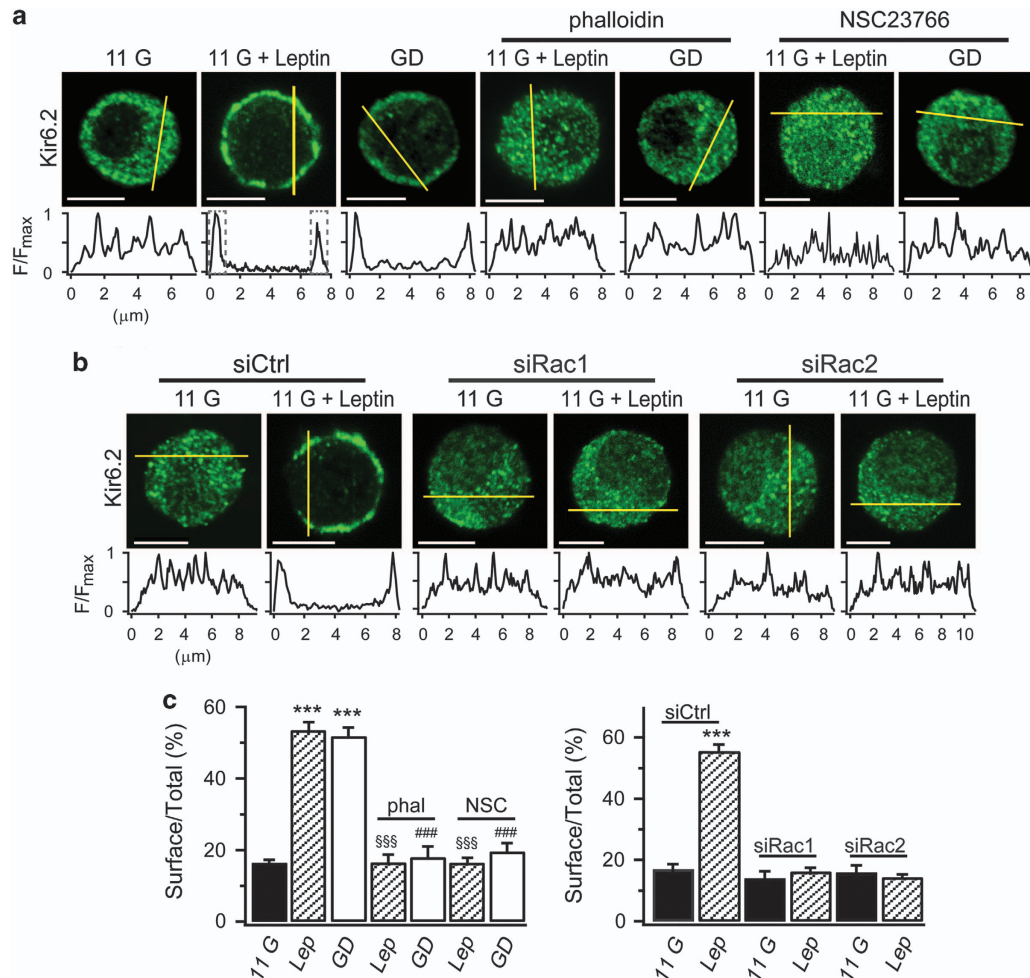
**Figure 3** AMPK-induced K$_{ATP}$ channel trafficking is inhibited by Rac inhibition. (**a**) Immunofluorescence analysis of the subcellular localization of K$_{ATP}$ channels in INS-1 cells using anti-Kir6.2 antibody in the presence of 11 mM glucose (11 G), 10 nM leptin in 11 G (11 G+Leptin), 0 mM glucose (GD), leptin and 10 μM phalloidin (phal) or 50 μM NSC23766 (NSC) in 11 G, and 10 μM phalloidin or 50 μM NSC23766 in GD. The yellow line across the cell used to measure Kir6.2 fluorescence intensity is shown underneath each image. Scale bar, 5 μm. (**b**) Experiments and analyses were the same as in (**a**), with the exception that the comparison was carried out in the absence or presence of leptin in siCtrl-, siRac1-, or siRac2-transfected cells. Scale bar, 5 μm. (**c**) Integration of the fluorescent intensities at the cell periphery (1 μm each, dashed line boxes) reflects the surface density of Kir6.2. Surface localization of Kir6.2 was expressed as the ratio of surface to total Kir6.2 fluorescence. Data are represented as the mean ± s.e.m. ($n$ = 5-24). ***$P$ < 0.001 compared with 11 G. §§§$P$ < 0.001 compared with Leptin (Lep). ###$P$ < 0.001 compared with GD.

siAMPK-treated cells. We found that leptin markedly increased MRLC phosphorylation in scrambled RNA-infected cells, and this increase was abolished in siAMPK-transfected cells (Figure 6a). Because MRLC phosphorylation is determined by the balance between a myosin light chain kinase and a myosin light chain phosphatase (MLCP), either the activation of myosin light chain kinase or the inactivation of MLCP causes increased MRLC phosphorylation.[27] Because MLCP is inactivated by its phosphorylation,[28,29] we tested the possibility that AMPK activation increases inhibitory phosphorylation of MLCP using western blot analysis in the same set of experiments that were used to measure the level of phosphorylated MRLC. The level of pMLCP was increased in leptin-treated cells, indicating that MLCP inactivation by AMPK activation is attributable to the increased MRLC phosphorylation (Figure 6a).

We then investigated whether MRLC is involved in AMPK-induced K$_{ATP}$ channel trafficking. When surface levels of Kir6.2 were assessed by surface biotinylation and western blot analysis in control and siMRLC-treated cells, the leptin-induced increase in the surface levels of Kir6.2 was abolished in siMRLC-treated cells, whereas total levels of Kir6.2 were not affected (Figure 6b). Immunocytochemical studies showed that siMRLC also suppressed leptin-induced K$_{ATP}$ channel trafficking to surface membrane (Figure 6c). However, increasing the phosphorylation of MRLC by calyculin A (50 nM), an MLCP inhibitor, did not induce K$_{ATP}$ channel trafficking (Supplementary Figure 2). These results indicate that MRLC phosphorylation induced by AMPK activation is required, but not sufficient, for K$_{ATP}$ channel trafficking.
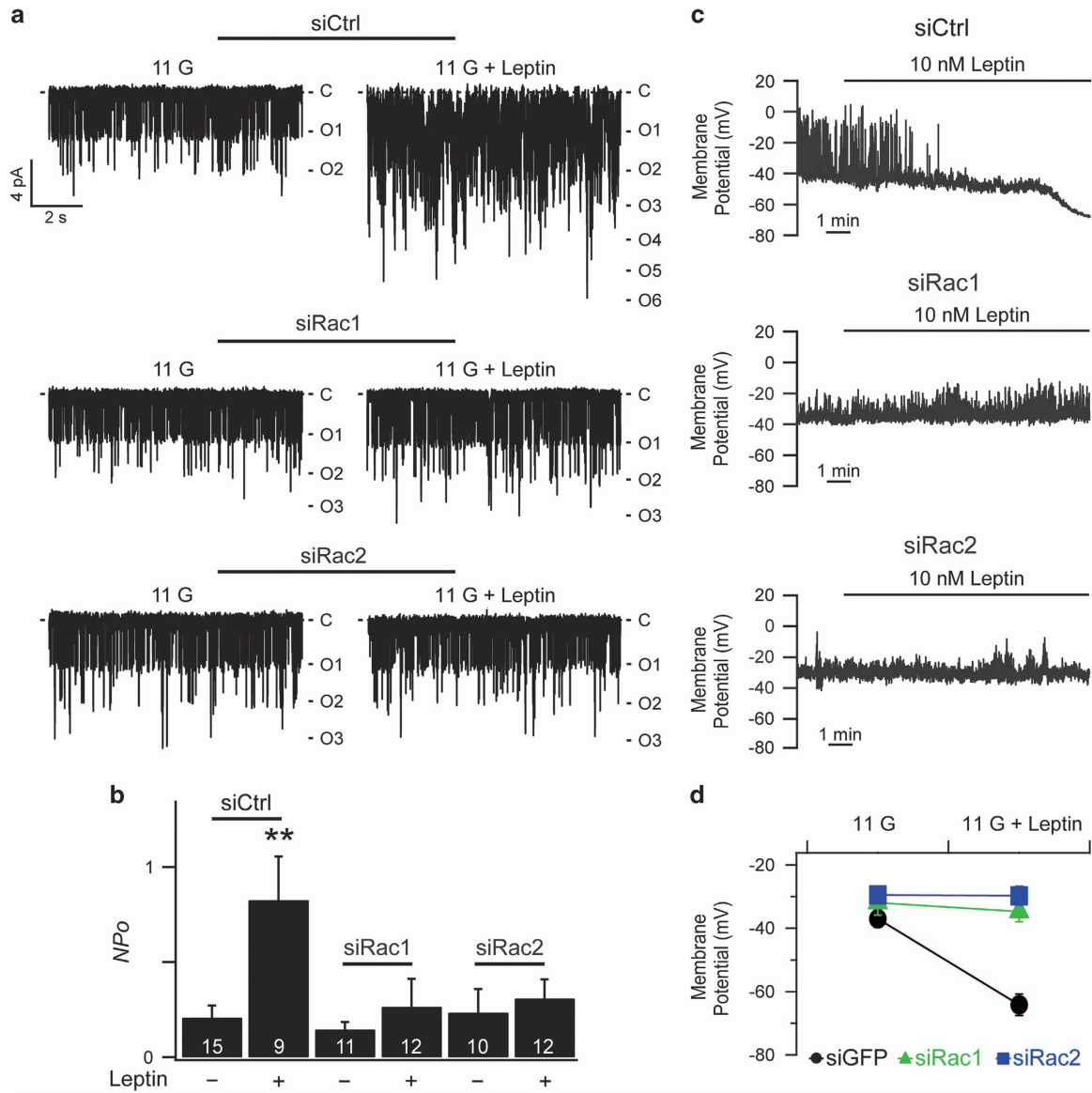
**Figure 4** Rac knockdown inhibits the leptin-induced increase in K$_{ATP}$ channel activity and leptin-induced hyperpolarization. (**a**) Representative single K$_{ATP}$ channel currents of siCtrl-, siRac1-, or siRac2-transfected INS-1 cells pretreated with or without 10 nm leptin. The inside-out patches were held at $-60$ mV. C, closed level. O, opened level. (**b**) Mean K$_{ATP}$ channel activity (*NPo*) of siCtrl-, siRac1-, or siRac2-transfected INS-1 cells pretreated with or without 10 nm leptin (siCtrl/11 G, 0.21±0.06, $n=15$; siCtrl/11 G+Leptin, 0.83±0.23, $n=9$; siRac1/11 G, 0.15±0.04, $n=11$; siRac1/11 G+Leptin, 0.27±0.15, $n=12$; siRac2/11 G, 0.24±0.12, $n=10$; siRac2/11 G+Leptin, 0.31±0.1, $n=12$). Data are represented as the mean±s.e.m. **$P<0.01$ compared with siCtrl/11 G. (**c**) Representative traces for the effects of leptin on membrane potentials from siCtrl-, siRac1-, or siRac2-transfected INS-1 cells. (**d**) Summary data for mean resting membrane potential (RMP) of INS-1 cells transfected with siCtrl, siRac1, or siRac2 before or after the application of leptin (siCtrl/11 G, $-37.0±2.6$ mV, $n=8$; siCtrl/11 G+Leptin, $-64.2±3.4$ mV, $n=8$; siRac1/11 G, $-32.0±3.9$ mV, $n=7$; siRac1/11 G+Leptin, $-34.7±3.2$ mV, $n=7$; siRac2/11 G, $-29.5±2.6$ mV, $n=8$; siRac2/11 G+Leptin, $-29.8±3.0$ mV, $n=8$). Data are represented as the mean±s.e.m.

## Myosin II mediates actin remodeling and K$_{ATP}$ channel trafficking by AMPK/Rac signaling

Because increased MRLC phosphorylation leads to the activation of MyoII, we investigated whether the involvement of MRLC in leptin-induced K$_{ATP}$ channel trafficking is attributable to the motor activity of MyoII. To assess the effects of inhibition of MyoII on leptin-induced K$_{ATP}$ channel trafficking, blebbistatin, a specific inhibitor of MyoII ATPase,[30] was used. We found that the leptin-induced increase in the surface levels of Kir6.2 was abolished by blebbistatin (50 μM), whereas the leptin-induced increase in MRLC phosphorylation was unaffected (Figure 7a). Consistent with that result, we also observed that blebbistatin inhibited leptin-induced K$_{ATP}$ channel trafficking to the surface using immunocytochemistry (Figure 7b). Furthermore, blebbistatin inhibited leptin-induced hyperpolarization (Figure 7c). Together, these results indicate
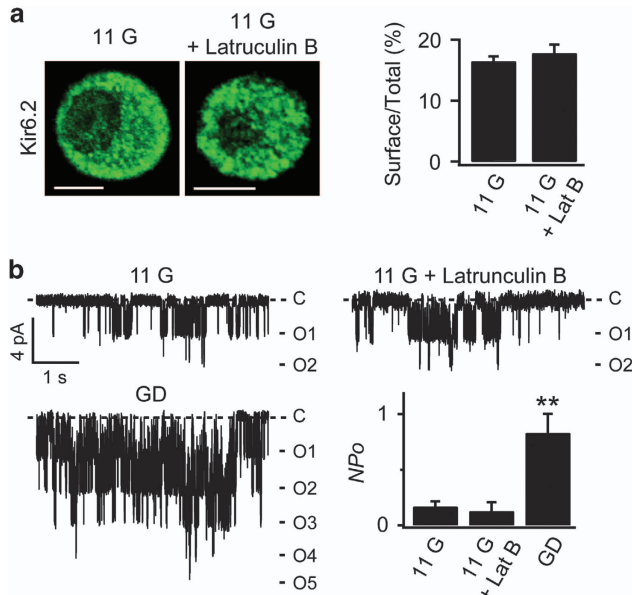
**Figure 5** Latrunculin B does not increase K_{ATP} channel activity and surface localization of Kir6.2. (**a**) Immunofluorescence analysis of the subcellular localization of K_{ATP} channels INS-1 cells using anti-Kir6.2 antibody in the absence or presence of 10 μM latrunculin B (Lat B) for 30 min in 11 mM glucose (left). Scale bar, 5 μm. Surface localization of Kir6.2 was expressed as the ratio of surface to total Kir6.2 fluorescence (right; 11 G, $n=24$; 11 G+Lat B, $n=3$). Data are represented as the mean ± s.e.m. (**b**) Representative single K_{ATP} channel currents of INS-1 cells 11G, 11G+Lat B, and GD. Mean K_{ATP} channel activity (*NPo*) in the absence and presence of latrunculin B (11 G, $0.16 \pm 0.05$, $n=14$; 11 G+Latrunculin B (Lat B), $0.13 \pm 0.08$, $n=10$). Data are represented as the mean ± s.e.m. \*\**P*<0.01 compared with 11 G +LatB.

that the increase in MyoII motor activity by MRLC phosphorylation plays a crucial role in the leptin-induced increase in K_{ATP} channel trafficking and hyperpolarization in pancreatic β-cells.

Because we found that K_{ATP} channel trafficking is closely associated with actin remodeling, the next question was the nature of the relationship between MyoII activation and actin remodeling. We found that blebbistatin inhibited leptin-induced actin depolymerization, and dense cortical actin was observed in blebbistatin-treated INS-1 cells in the presence of leptin (Figure 7d), supporting a role of MyoII in AMPK-dependent actin remodeling.

Consistent with the above results, inhibition of MyoII by siMRLC or blebbistatin inhibited the effects of GD on K_{ATP} channel activity, K_{ATP} channel trafficking and actin remodeling (Supplementary Figure 3). We also confirmed the specificity of blebbistatin as a MyoII ATPase inhibitor by showing that inactive blebbistatin had no effect on K_{ATP} channel trafficking and actin remodeling by GD (Supplementary Figures 3c and d). These data support the notion that MyoII has an important role in AMPK-dependent K_{ATP} channel trafficking and actin remodeling.
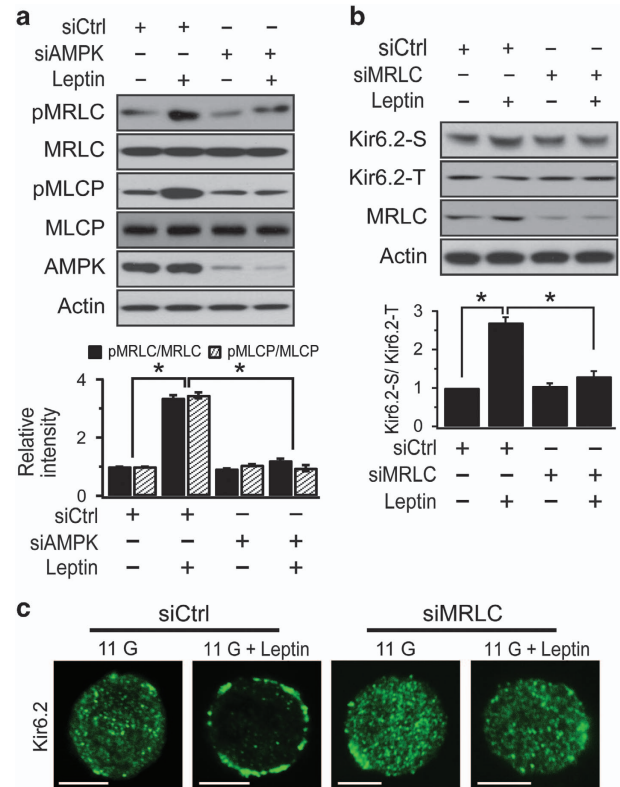


**Figure 6** MRLC phosphorylation is involved in leptin-induced K_{ATP} channel trafficking. (**a**) Reduction of leptin-induced MRLC and MLCP phosphorylation by knockdown of AMPK. INS-1 cells were transfected with siCtrl or siAMPK for 48 h and then treated with leptin at 10 nM for 30 min before western blot analysis. The relative ratio of phosphorylated MRLC or MLCP and total MRLC or MLCP was plotted based on the quantification of the band intensities. The data are expressed as the mean ± s.e.m. ($n=3$). \**P*<0.05 compared as indicated. (**b**) Suppression of K_{ATP} channel trafficking by knockdown of MRLC. Cells were transfected with siCtrl or siMRLC for 48 h and then treated with leptin at 10 nM for 30 min prior to surface labeling with a biotin probe. The relative ratio of surface to total Kir6.2 was plotted based on the quantification of the band intensities. The data are expressed as the mean ± s.e.m. ($n=3$). \**P*<0.05 compared as indicated. (**c**) Effect of MRLC knockdown on immunostaining of Kir6.2 before and after lepin treatment in INS-1 cells. The cells were transfected with siCtrl or siMRLC for 48 h and then treated with leptin for 30 min before immunofluorescence analysis using anti-Kir6.2 antibody. Scale bar, 5 μm.

We showed that both Rac and MRLC are downstream of AMPK activation and involved in K_{ATP} channel trafficking and actin remodeling, leading us to question the relationship between Rac activation and MRLC phosphorylation. To this end, we measured the effect of a Rac inhibitor, NSC23766, on the leptin-induced increase in pMRLC levels, and found that Rac inhibition blocked the increase in MRLC phosphorylation by leptin (Figure 8a). This result suggested that AMPK/Rac activation is upstream of MRLC phosphorylation.

We previously reported that PTEN inactivation is involved in AMPK-dependent K_{ATP} channel trafficking.[31] Thus, the last
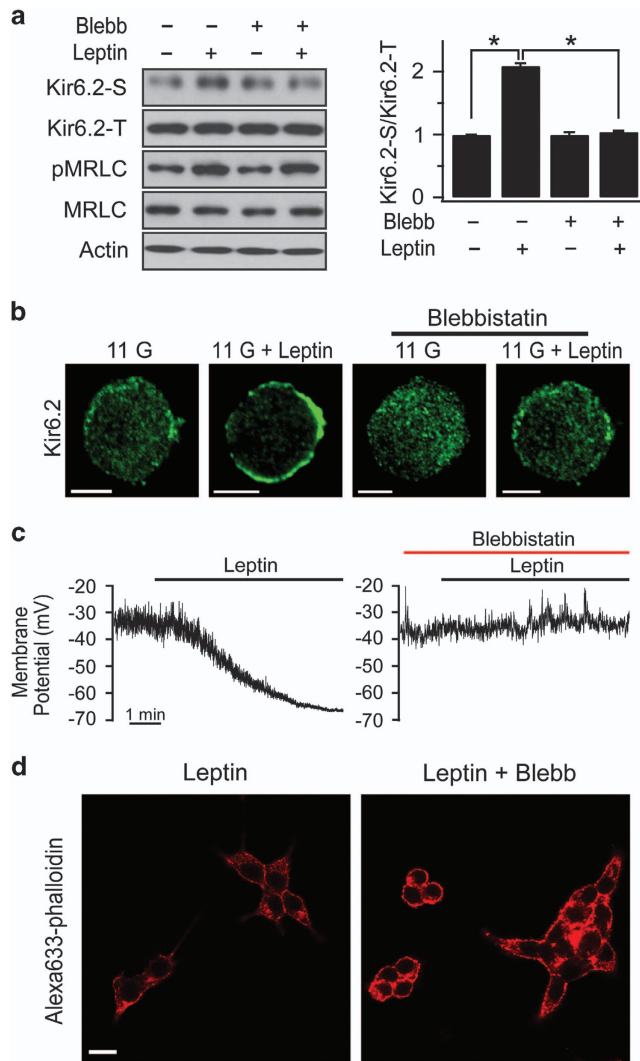
**Figure 7** MyoII activity is crucial for K$_{ATP}$ channel trafficking. (**a**) Effect of blebbistatin, an inhibitor of MyoII, on leptin-induced K$_{ATP}$ channel trafficking and MRLC phosphorylation. INS-1 cells were treated with leptin and/or 50 μM blebbistatin (Blebb) for 30 min before surface labeling with a biotin probe. The relative ratio of surface to total Kir6.2 was plotted based on the quantification of the band intensities. The data are expressed as the mean ± s.e.m. (*n* = 3). *P < 0.05 compared as indicated. (**b**) Effect of blebbistatin on Kir6.2 immunostaining before and after leptin treatment in INS-1 cells. Scale bars, 5 μm. (**c**) Representative traces for the effects of blebbistatin on membrane potentials from leptin-treated INS-1 cells. Leptin-induced hyperpolarization was abolished in the presence of 50 μM blebbistatin. (**d**) Confocal fluorescent images of F-actin staining with Alexa 633-phalloidin in INS-1 cells pretreated with 10 nM leptin and 50 μM blebbistatin (Blebb) in 11 mM glucose. Scale bars, 10 μm.

question to address was whether PTEN inactivation is upstream of Rac/MyoII activation. To test this possibility, we investigated whether PTEN inhibition is sufficient to increase MRLC phosphorylation by using a dominant-negative mutant of PTEN (PTEN$^{C124S}$), which is defective in both lipid and protein phosphatase activity.[32] Overexpression of PTEN$^{C124S}$ increased MRLC phosphorylation and MLCP phosphorylation
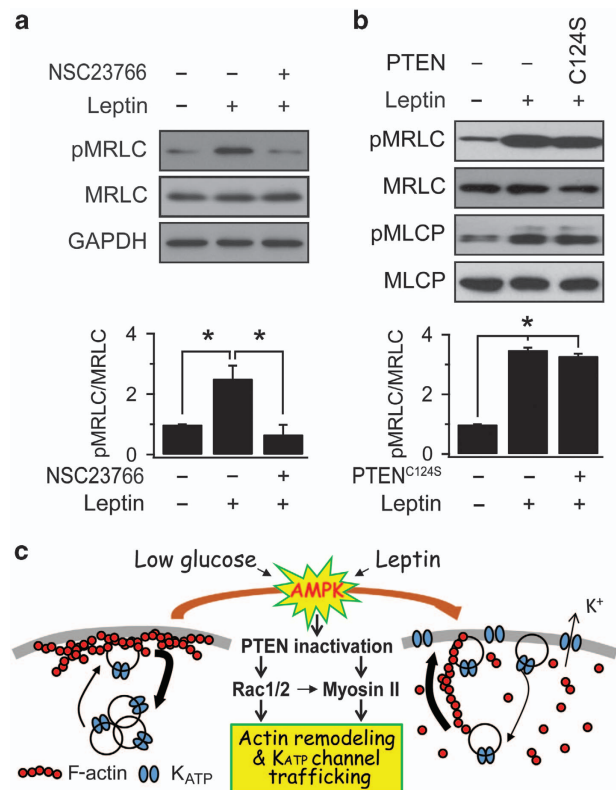


**Figure 8** PTEN inactivation and Rac are upstream of MRLC phosphorylation. (**a**) Effect of the Rac inhibitor (NSC23766) on the lepin-induced increase of MRLC phosphorylation. Cells were treated with leptin or leptin and 50 μM NSC23766 for 30 min prior to western blot analysis. The relative ratio of phosphorylated MRLC to total MRLC was plotted based on the quantification of the band intensities. The data are expressed as the mean ± s.e.m. (*n* = 3). *P < 0.05 compared as indicated. (**b**) The change in MRLC phosphorylation by PTEN inactivation. The cells were transfected with PTEN$^{WT}$ (wild-type PTEN) or PTEN$^{C124}$ construct (a lipid and protein phosphatase dead form of PTEN) for 48 h. The relative ratio of phosphorylated MRLC to total MRLC was plotted based on the quantification of the band intensities. The data are expressed as the mean ± s.e.m. (*n* = 3). *P < 0.05 compared as indicated. (**c**) Schematic illustration of signaling pathways underlying K$_{ATP}$ channel trafficking induced by GD or leptin revealed by the present and previous studies.[2,4,31]

to the level induced by leptin treatment (Figure 8b). We also confirmed that overexpression of PTEN$^{C124S}$ induced activation of Rac1 and Rac2 (Supplementary Figure 4). These results support the notion that PTEN inactivation is upstream of Rac/MyoII activation. The signaling pathways involved in AMPK-dependent K$_{ATP}$ channel trafficking shown in our present and previous papers[2,4,31] are summarized in Figure 8c.

## DISCUSSION

The K$_{ATP}$ channel has a crucial role in the maintenance of glucose homeostasis by regulating insulin secretion. Studies of the regulation of K$_{ATP}$ channel activity provide fundamental information for establishing strategies that improve impaired insulin secretion in diabetes mellitus.[33,34] Because

10

the mechanisms for direct regulation of K$_{ATP}$ channel gating have been well established,[35] we focused on how K$_{ATP}$ channel translocation to the plasma membrane is regulated. We demonstrated that both GD and leptin activate AMPK to promote K$_{ATP}$ channel trafficking to the surface of pancreatic β-cells and that K$_{ATP}$ channel density and β-cell membrane potentials are correlated with phospho-AMPK levels.[2,4] We then identified the involvement of PTEN inactivation mediated by GSKβ activation as a downstream molecular target of AMPK that leads to K$_{ATP}$ channel trafficking.[31] In the present study, we found a close association of actin remodeling and AMPK-dependent K$_{ATP}$ channel trafficking and identified Rac GTPase and MyoII as key molecules that mediate actin remodeling and K$_{ATP}$ channel trafficking.

The relationship between Rac-dependent actin remodeling and cell signal-dependent trafficking of membrane proteins has been thoroughly investigated in studies of GLUT4 glucose transporter trafficking in response to insulin signaling. GLUT4, expressed highly in adipose and muscle tissues, serves as a key component in regulating glucose homeostasis by undergoing translocation to the plasma membrane and uptaking glucose after insulin stimulation and exercise.[36] Previous studies have found that insulin-dependent GLUT4 translocation is dependent on actin remodeling; actin depolymerizing agents, such as swinholide-A, latrunculin B and jasplakinolide, an actin filament polymerizing and stabilizing drug, inhibited insulin-stimulated actin rearrangement and GLUT4 translocation in muscle cells[37] and adipocytes.[38] Recent studies showed that the overexpression of the dominant inhibitory Rac1 mutant or siRac1 prevented insulin-induced actin remodeling and GLUT4 translocation.[11,25] Further studies revealed the involvement of the branching complex Arp2/3, the severing protein cofilin,[39] and tropomodulin3[40] in GLUT4 translocation. Furthermore, the possibility of a link between AMPK and Rac signaling in GLUT4 translocation was also suggested by the effects of retinoic acid on skeletal muscle cells.[41] Altogether, these studies claimed that cortical actin remodeling provides a track for moving GLUT4-containing vesicles to the cell surface. In general, Rac-mediated actin remodeling induced by insulin signaling in adipocytes and myocytes is associated with actin polymerization.[25,26] However, insulin does not induce cytoskeletal remodeling in pancreatic β-cells or in hypothalamic cells where leptin induces actin depolymerization.[32] We also showed that Rac-mediated actin remodeling induced by AMPK signaling in pancreatic β-cells was manifested mainly by actin depolymerization (Figures 1 and 2 and Supplementary Figure 1b). Our results appear to be consistent with the idea that cortical F-actin in pancreatic β-cells acts as a physical barrier that obstructs K$_{ATP}$ channel trafficking and that depolymerization of F-actin is required for the translocation of K$_{ATP}$ channels to the surface membrane. Consistent with this idea, increased surface expression of SUR1 by the actin depolymerizing agent latrunculin B was reported.[10] We, however, found that latrunculin B failed to induce K$_{ATP}$ channel trafficking or increased K$_{ATP}$ channel activity (Figure 5). We do not know the reason for the difference

between these two studies, but our results imply that simple destruction of barrier is not sufficient; rather, a more active process is involved in K$_{ATP}$ channel trafficking.

We also provided evidence for the contribution of MyoII in actin remodeling and K$_{ATP}$ channel trafficking induced by AMPK signaling. We showed that the AMPK-induced increase in K$_{ATP}$ channel trafficking is not only dependent on MRLC phosphorylation but is also inhibited by blockade of MyoII ATPase (Figures 6b and 7a), indicating that the motor activity of MyoII is required for K$_{ATP}$ channel trafficking. Involvement of MyoII in insulin-dependent GLUT4 vesicle translocation has been well studied, and there are similarities and differences between GLUT4 and K$_{ATP}$ channel trafficking. GLUT4 translocates to the plasma membrane prior to MyoII activation, and the co-localization of MyoII and GLUT4 is required for proper fusion of GLUT4-vesicles.[42] By contrast, our immunocytochemistry results show that the inhibition of MyoII inhibits the translocation of K$_{ATP}$ channel to the plasma membrane (Figures 6 and 7 and Supplementary Figure 3). MyoII activation is commonly mediated by increased phosphorylation of MRLC, but there is a difference in the mechanism of MRLC phosphorylation. MRLC phosphorylation in insulin signaling is mediated by Ca$^{2+}$/calmodulin-dependent activation of myosin light chain kinase,[42] whereas MRLC phosphorylation in AMPK signaling is mediated by inhibitory phosphorylation of MLCP (Figure 6a) induced by PTEN inactivation (Figure 8b). In insulin-dependent GLUT4 translocation, recruitment of F-actin to the plasma membrane is an important step, and MyoII was shown to be necessary for F-actin localization.[20] By contrast, we showed in the present study that disruption of cortical actin is required for K$_{ATP}$ channel trafficking, and MyoII has a key role in actin depolymerization as well as in K$_{ATP}$ channel trafficking in pancreatic β-cells. There are several reports that support the role of MyoII in actin depolymerization in various tissues. The inhibition of MyoII ATPase activity with blebbistatin prevented actin turnover in mammalian cultured cells.[43] Myosin II has a role in actin network disassembly in migrating fish keratocytes.[44] Another recent study showed a role of MyoII in disassembly of F-actin for actomyosin ring constriction.[45] These studies support the role of MyoII in promoting actin depolymerization. However, we do not think that the activation of MyoII alone is enough to induce actin remodeling and K$_{ATP}$ channel trafficking because we failed to induce these changes by inhibiting MLCP with calyculin A (Supplementary Figure 2). It is thus reasonable to conclude that actin remodeling mediated by the coordinated actions of Rac signaling and MyoII leads to the translocation of K$_{ATP}$ channel-containing vesicles to the plasma membrane.

In pancreatic β-cells, the role of the cytoskeleton in regulating vesicle trafficking has been extensively studied in glucose-stimulated insulin secretion. High glucose stimulation causes depolymerization of cortical actin, leading to insulin secretion.[13,46,47] This was supported by the enhanced glucose-stimulated insulin secretion following the application of actin-disrupting agents.[46,48,49] Furthermore, glucose-induced

translation of Rac1 to the membrane and Rac1 activation were proposed to contribute to glucose-dependent actin depolymerization and insulin secretion.[13,50,51] Actin depolymerization by high glucose appears to contradict our results, but in glucose-stimulated insulin secretion, F-actin remodeling by high glucose was observed after 5 min stimulation and recovered within 30 min.[46] In our study, dense cortical rings of F-actin were observed in INS-1 cells incubated in 11 mM glucose, and F-actin was disrupted when AMPK was activated by GD or leptin treatment. These results may suggest that actin depolymerization induced by high glucose is an acute and transient process that facilitates the translocation of insulin-containing vesicles in the initial step of glucose-stimulated insulin secretion, but at steady state in high glucose conditions, cortical actin is restored. When cells are exposed to energy deprived conditions, cytoskeletal remodeling occurs again but via different signaling mechanisms; AMPK/Rac/MyoII activation couples cytoskeletal remodeling to the translocation of K$_{ATP}$ channels. The question remains as to how Rac mediates cytoskeletal remodeling in such opposite directions and how it regulates the translocation of different targets. These questions remain to be investigated in future studies.

In conclusion, the aim of this study was to understand the implications of Rac-dependent actin dynamics in AMPK-dependent K$_{ATP}$ channel trafficking in pancreatic β-cells. We demonstrated that AMPK/Rac-induced actin depolymerization, which is mediated by MyoII through phosphorylation of MRLC, is required for K$_{ATP}$ channel trafficking to the surface membrane in pancreatic β-cells.

## CONFLICT OF INTEREST

The authors declare no conflict of interest.

1 Leibiger IB, Leibiger B, Berggren PO. Insulin signaling in the pancreatic β-cell. *Annu Rev Nutr* 2008; **28**: 233–251.
2 Park SH, Ryu SY, Yu WJ, Han YE, Ji YS, Oh K et al. Leptin promotes K$_{ATP}$ channel trafficking by AMPK signaling in pancreatic β-cells. *Proc Natl Acad Sci USA* 2013; **110**: 12673–12678.
3 Kahn BB, Alquier T, Carling D, Hardie DG. AMP-activated protein kinase: ancient energy gauge provides clues to modern understanding of metabolism. *Cell Metab* 2005; **1**: 15–25.
4 Lim A, Park SH, Sohn JW, Jeon JH, Park JH, Song DK et al. Glucose deprivation regulates K$_{ATP}$ channel trafficking via AMP-activated protein kinase in pancreatic β-cells. *Diabetes* 2009; **58**: 2813–2819.
5 Lee JH, Koh H, Kim M, Kim Y, Lee SY, Karess RE et al. Energy-dependent regulation of cell structure by AMP-activated protein kinase. *Nature* 2007; **447**: 1017–1020.
6 Blume C, Benz PM, Walter U, Ha J, Kemp BE, Renné T. AMP-activated protein kinase impairs endothelial actin cytoskeleton assembly by phosphorylating vasodilator-stimulated phosphoprotein. *J Biol Chem* 2007; **282**: 4601–4612.
7 Malacombe M, Bader MF, Gasman S. Exocytosis in neuroendocrine cells: new tasks for actin. *Biochim Biophys Acta* 2006; **1763**: 1175–1183.
8 Johnson JL, Monfregola J, Napolitano G, Kiosses WB, Catz SD. Vesicular trafficking through cortical actin during exocytosis is regulated by the Rab27a effector JFC1/Slp1 and the RhoA-GTPase–activating protein Gem-interacting protein. *Mol Biol Cell* 2012; **23**: 1902–1916.
9 Lim A, Park SH, Lee SH, Ho WK. Actin depolymerization and myosin light chain phosphorylation underlie AMPK-induced K$_{ATP}$ channel trafficking in pancreatic β-cells. *Biophysical Society 54th Annual Meeting Pos-L208 Abstract*. Biophysical Society: Rockville, MD, USA, 2010.
10 Chen PC, Kryukova YN, Shyng SL. Leptin regulates K$_{ATP}$ channel trafficking in pancreatic β-cells by a signaling mechanism involving AMP-activated protein kinase (AMPK) and cAMP-dependent potein kinase (PKA). *J Biol Chem* 2013; **288**: 34098–34109.
11 JeBailey L, Wanono O, Niu W, Roessler J, Rudich A, Klip A. Ceramide- and oxidant-induced insulin resistance involve loss of insulin-dependent Rac-activation and actin remodeling in muscle cells. *Diabetes* 2007; **56**: 394–403.
12 Li J, Luo R, Kowluru A, Li G. Novel regulation by Rac1 of glucose- and forskolin-induced insulin secretion in INS-1 β-cells. *Am J Physiol Endocrinol Metab* 2004; **286**: E818–E827.
13 Asahara S, Shibutani Y, Teruyama K, Inoue HY, Kawada Y, Etoh H et al. Ras-related C3 botulinum toxin substrate 1 (RAC1) regulates glucose-stimulated insulin secretion via modulation of F-actin. *Diabetologia* 2013; **56**: 1088–1097.
14 Ikonen E, de Almeid JB, Fath KR, Burgess DR, Ashman K, Simons K et al. Myosin II is associated with Golgi membranes: identification of p200 as nonmuscle myosin II on Golgi-derived vesicles. *J Cell Sci* 1997; **110**: 2155–2164.
15 Müsch A, Cohen D, Rodriguez-Boulan E. Myosin II is involved in the production of constitutive transport vesicles from the TGN. *J Cell Biol* 1997; **138**: 291–306.
16 Dean SO, Rogers SL, Stuurman N, Vale RD, Spudich JA. Distinct pathways control recruitment and maintenance of myosin II at the cleavage furrow during cytokinesis. *Proc Natl Acad Sci USA* 2005; **102**: 13473–13478.
17 Medeiros NA, Burnette DT, Forscher P. Myosin II functions in actin-bundle turnover in neuronal growth cones. *Nat Cell Biol* 2006; **8**: 216–226.
18 Choi YO, Ryu HJ, Kim HR, Song YS, Kim C, Lee W et al. Implication of phosphorylation of the myosin II regulatory light chain in insulin-stimulated GLUT4 translocation in 3T3-F442A adipocytes. *Exp Mol Med* 2006; **38**: 180–189.
19 Lee JS, Kim MH, Ho WK, Lee SH. Presynaptic release probability and readily releasable pool size are regulated by two independent mechanisms during posttetanic potentiation at the calyx of Held synapse. *J Neurosci* 2008; **28**: 7945–7953.
20 Stall R, Ramos J, Kent Fulcher F, Patel YM. Regulation of myosin IIA and filamentous actin during insulin-stimulated glucose uptake in 3T3-L1 adipocytes. *Exp Cell Res* 2014; **322**: 81–88.
21 Lee CS, Choi CK, Shin EY, Schwartz MA, Kim EG. Myosin II directly binds and inhibits Dbl family guanine nucleotide exchange factors: a possible link to Rho family GTPases. *J Cell Biol* 2010; **190**: 663–674.
22 Shin EY, Lee CS, Yun CY, Won SY, Kim HK, Lee YH et al. Non-muscle myosin II regulates neuronal actin dynamics by interacting with guanine nucleotide exchange Factors. *PLoS One* 2014; **9**: e95212.
23 Kalwat MA, Thurmond DC. Signaling mechanisms of glucose-induced F-actin remodeling in pancreatic islet β cells. *Exp Mol Med* 2013; **45**: e37.
24 Hall A. Rho GTPases and the actin cytoskeleton. *Science* 1998; **279**: 509–514.
25 Khayat ZA, Tong P, Yaworsky K, Bloch RJ, Klip A. Insulin-induced actin filament remodeling colocalizes actin with phosphatidylinositol 3-kinase and GLUT4 in L6 myotubes. *J Cell Sci* 2000; **113**: 279–290.
26 Balamatsias D, Kong AM, Waters JE, Sriratana A, Gurung R, Bailey CG et al. Identification of P-Rex1 as a novel Rac1-guanine nucleotide exchange factor (GEF) that promotes actin remodeling and GLUT4 protein trafficking in adipocytes. *J Biol Chem* 2011; **286**: 43229–43240.
27 Somlyo AP, Somlyo AV. Ca$^{2+}$ sensitivity of smooth muscle and nonmuscle myosin II: modulated by G proteins, kinases, and myosin phosphatase. *Physiol Rev* 2003; **83**: 1325–1358.
28 Kimura K, Ito M, Amano M, Chihara K, Fukata Y, Nakafuku M et al. Regulation of myosin phosphatase by Rho and Rho-associated kinase (Rho-kinase). *Science* 1996; **273**: 245–248.
29 Murányi A, Derkach D, Erdődi F, Kiss A, Ito M, Hartshorne DJ. Phosphorylation of Thr695 and Thr850 on the myosin phosphatase target subunit: inhibitory effects and occurrence in A7r5 cells. *FEBS Lett* 2005; **579**: 6611–6615.
30 Straight AF, Cheung A, Limouze J, Chen I, Westwood NJ, Sellers JR et al. Dissecting temporal and spatial control of cytokinesis with a myosin II inhibitor. *Science* 2003; **299**: 1743–1747.
31 Park SH, Ho WK, Jeon JH. AMPK regulates K$_{ATP}$ channel trafficking via PTEN inhibition in leptin-treated pancreatic β-cells. *Biochem Biophys Res Commun* 2013; **440**: 539–544.

32 Ning K, Miller LC, Laidlaw HA, Burgess LA, Perera NM, Downes CP *et al.* A novel leptin signalling pathway via PTEN inhibition in hypothalamic cell lines and pancreatic β-cells. *EMBO J* 2006; **25**: 2377–2387.

33 Nichols CG. K$_{ATP}$ channels as molecular sensors of cellular metabolism. *Nature* 2006; **440**: 470–476.

34 McTaggart JS, Clark RH, Ashcroft FM. The role of the K$_{ATP}$ channel in glucose homeostasis in health and disease: more than meets the islet. *J Physiol* 2010; **588**: 3201–3209.

35 Enkvetchakul D, Nichols CG. Gating mechanism of K$_{ATP}$ channels: function fits form. *J Gen Physiol* 2003; **122**: 471–480.

36 Huang S, Czech MP. The GLUT4 glucose transporter. *Cell Metab* 2007; **5**: 237–252.

37 Tong P, Khayat ZA, Huang C, Patel N, Ueyama A, Klip A. Insulin-induced cortical actin remodeling promotes GLUT4 insertion at muscle cell membrane ruffles. *J Clin Invest* 2001; **108**: 371–381.

38 Kanzaki M, Pessin JE. Insulin-stimulated GLUT4 translocation in adipocytes is dependent upon cortical actin remodeling. *J Biol Chem* 2001; **276**: 42436–42444.

39 Chiu TT, Patel N, Shaw AE, Bamburg JR, Klip A. Arp2/3- and Cofilin-coordinated actin dynamics is required for insulin-mediated GLUT4 translocation to the surface of muscle cells. *Mol Biol Cell* 2010; **21**: 3529–3539.

40 Lim CY, Bi X, Wu D, Kim JB, Gunning PW, Hong W *et al.* Tropomodulin3 is a novel Akt2 effector regulating insulin-stimulated GLUT4 exocytosis through cortical actin remodeling. *Nat Commun* 2015; **6**: 5951.

41 Lee YM, Lee JO, Jung JH, Kim JH, Park SH, Park JM *et al.* Retinoic acid leads to cytoskeletal rearrangement through AMPK-Rac1 and stimulates glucose uptake through AMPK-p38 MAPK in skeletal muscle cells. *J Biol Chem* 2008; **283**: 33969–33974.

42 Fulcher FK, Smith BT, Russ M, Patel YM. Dual role for myosin II in GLUT4-mediated glucose uptake in 3T3-L1 adipocytes. *Exp Cell Res* 2008; **314**: 3264–3274.

43 Guha M, Zhou M, Wang YL. Cortical actin turnover during cytokinesis requires myosin II. *Curr Biol* 2005; **15**: 732–736.

44 Wilson CA, Tsuchida MA, Allen GM, Barnhart EL, Applegate KT, Yam PT *et al.* Myosin II contributes to cell-scale actin network treadmilling through network disassembly. *Nature* 2010; **465**: 373–377.

45 Mendes Pinto I, Rubinstein B, Kucharavy A, Unruh JR, Li R. Actin depolymerization drives actomyosin ring contraction during budding yeast cytokinesis. *Dev Cell* 2012; **22**: 1247–1260.

46 Thurmond DC, Gonelle-Gispert C, Furukawa M, Halban PA, Pessin JE. Glucose-stimulated insulin secretion is coupled to the interaction of actin with the t-SNARE (target membrane soluble N-ethylmaleimide-sensitive factor attachment protein receptor protein) complex. *Mol Endocrinol* 2003; **17**: 732–742.

47 Nevins AK, Thurmond DC. Glucose regulates the cortical actin network through modulation of Cdc42 cycling to stimulate insulin secretion. *Am J Physiol Cell Physiol* 2003; **285**: C698–C710.

48 Wang JL, Easom RA, Hughes JH, McDaniel ML. Evidence for a role of microfilaments in insulin release from purified β-cells. *Biochem Biophys Res Commun* 1990; **171**: 424–430.

49 Li G, Rungger-Brändle E, Just I, Jonas JC, Aktories K, Wollheim CB. Effect of disruption of actin filaments by Clostridium botulinum C2 toxin on insulin secretion in HIT-T15 cells and pancreatic islets. *Mol Biol Cell* 1994; **5**: 1199–1213.

50 Veluthakal R, Kaur H, Goalstone M, Kowluru A. Dominant-negative α-subunit of farnesyl- and geranyltransferase inhibits glucose-stimulated, but not KCl-stimulated, insulin secretion in INS 832/13 cells. *Diabetes* 2007; **56**: 204–210.

51 Veluthakal R, Madathilparambil SV, McDonald P, Olson LK, Kowluru A. Regulatory roles for Tiam1, a guanine nucleotide exchange factor for Rac1, in glucose-stimulated insulin secretion in pancreatic β-cells. *Biochem Pharmacol* 2009; **77**: 101–113.

Supplementary Information accompanies the paper on Experimental & Molecular Medicine website (http://www.nature.com/emm)